Organotin(IV) Derivatives of Some O,C,O-Chelating Ligands. Part 2[⊥]

Libor Dostál,[†] Roman Jambor,[†] Aleš Růžička,*[,†] Ivana Císařová,[‡] Jaroslav Holeček,[†] Monique Biesemans,[§] Rudolph Willem,[§] Frank De Proft,[||] and Paul Geerlings[||]

Department of General and Inorganic Chemistry, Faculty of Chemical Technology, University of Pardubice, nám. Čs. legií 565, CZ-532 10, Pardubice, Czech Republic, Charles University in Prague, Faculty of Science, Hlavova 2030, 128 40 Praha 2, Czech Republic, and High Resolution NMR Centre (HNMR), Department of Materials and Chemistry (MACH), Faculty of Engineering, and Eenheid Algemene Chemie (ALGC), Department of Chemistry (DSCH), Faculty of Sciences, Vrije Universiteit Brussel (VUB), Pleinlaan 2, B-1050 Brussels, Belgium

Received June 12, 2007

A new O,C,O-chelating ligand $[2,6\text{-}C_6H_3(CH_2OEt)_2]^-$ and its organotin(IV) derivatives, $LSnPh_3$, $LSnPh_2Cl$, and $LSnPhCl_2$ (**4**−**6**), were prepared and structurally characterized in solution as well as in the solid state by NMR and XRD techniques. The structure of these compounds was compared to those of analogous compounds containing ligands of the type $[2,6\text{-}C_6H_3(CH_2OR)_2]^-$, where R = Me, *i*-Pr, and *t*-Bu, on the basis of various NMR spectral parameters, mainly on $^nJ(^1H-^{119}Sn)$ long-range couplings, solid-state structure determinations, and theoretical calculations at the B3LYP/LANL2DZ level. All of these methods showed that the structure is similar in all three phases (solid, solution, and in silico), but that it dramatically depends on the R substituent in the O,C,O-pincer ligand.

Introduction

The use of chelating, especially "pincer", ligands for the stabilization of coordinative metal centers in organometallic compounds is well documented.[1] These ligands have been applied to a class of organotin compounds as well.[2] Recently, we reported the synthesis of three monoanionic O,C,O-pincer ligands and their organotin derivatives.[3a] We investigated their solid-state structures, using XRD and CP/MAS NMR, as well as the solution-state structures of 11 compounds, including **1**−**3** and **7**−**12** (Scheme 1), using multinuclear NMR techniques. The structures of the 11 compounds mentioned were found to be similar in solution and in the solid state, with the tin atom varying from a tetrahedral 4-coordinate to an octahedral 6-coordinate configuration upon going from tetra- to monoorganotin compounds.[3a] The deviations from the ideal coordination polyhedral shapes depend on the degree of donor−acceptor Sn−O interactions, going from very weak to medium-strong. This interaction increases with increasing Lewis acidity of the tin atom, but decreases with increasing steric demands of the R substituents in the O,C,O-chelating ligands. In the compounds investigated, the Sn−O distances (2.475−2.966 Å) are substantially smaller than the sum of the van der Waals radii of oxygen and tin (3.70 Å),[4] but larger than the sum of the covalent radii (2.066 Å).[4] The carbon and/or chlorine atoms occupy the axial positions in the tin coordination sphere. The donor O-atoms coordinate to the tin atom with a O−Sn−O cis configuration resulting in a pseudofacial O,C,O-coordination mode of the "pincer" ligands. This cis configuration is retained, even in diorganotin compounds **3**, **9**, and **12**, in contrast to related diorganotin dichlorides containing another O,C,O-pincer ligand, the $5\text{-}t\text{-Bu-}1,3\text{-}C_6H_2[P(O)(OEt)_2]_2$ one, in which the oxygen atoms coordinate to the tin atom in a trans configuration.[5] Solution NMR spectra indicate similar structural arrangements around tin in solution and in the solid state, but direct data for the estimation of the strength of the Sn−O interactions in solution are missing so far. The measurement of long-range coupling constants appears to be a possibility to obtain this information.

This Article describes the measurement of long-range coupling constants in the series of organotin compounds **1**−**12**

[⊥] Dedicated to Assoc. Prof. Dr. Jaromír Plešek on the occasion of his 80th birthday in recognition of his outstanding contributions to the area of borane and carbaborane cluster chemistry.

* Corresponding author. Fax: + 420 46 603 7068. E-mail: ales.ruzicka@upce.cz.

[†] University of Pardubice.

[‡] Charles University in Prague.

[§] Department of Materials and Chemistry, Vrije Universiteit Brussel.

[||] Department of Chemistry, Vrije Universiteit Brussel.

(1) (a) *Chemistry of Hypervalent Compounds*; Akiba, K., Ed.; Wiley VCH: Weinheim, Germany, 1999; and references therein. (b) Jastrzebski, J. T. B. H.; Boersma, J.; Esch, P. M.; van Koten, G. *Organometallics* **1991**, *10*, 930. (c) Mitzel, N. W.; Losehand, U.; Richardson, A. *Organometallics* **1999**, *18*, 2610. (d) Buntine, M. A.; Kosovel, F. J.; Tiekink, E. R. T. *Phosphorus, Sulfur Silicon Relat. Elem.* **1999**, *150*−*151*, 261 and references therein. (e) van Koten, G.; Albrecht, M. *Angew. Chem., Int. Ed.* **2001**, *40*, 3750. (f) Holmes, R. R. *Chem. Rev.* **1990**, *90*, 17. (g) Corriu, R. J. P.; Mix, A.; Lanneau, G. F. *J. Organomet. Chem.* **1998**, *570*, 183. (h) Carré, F.; Chauhan, M.; Chuit, C.; Corriu, R. J. P.; Reyé, C. *J. Organomet. Chem.* **1997**, *540*, 175. (i) Carré, F.; Chuit, C.; Corriu, R. J. P.; Mehdi, A.; Reyé, C. *Organometallics* **1995**, *14*, 2754. (j) Chauhan, M.; Chuit, C.; Corriu, R. J. P.; Mehdi, A.; Reyé, C. *Organometallics* **1996**, *15*, 4326. (k) Chuit, C.; Corriu, R. J. P.; Mehdi, A.; Reyé, C. *Chem.-Eur. J.* **1996**, *2*, 342.

(2) (a) Jastrzebski, J. T. B. H.; van Koten, G. *Adv. Organomet. Chem.* **1993**, *35*, 241. (b) *Chemistry of Tin*; Smith, P. J., Ed.; Blackie Academic & Professional: Glasgow, U.K., 1998.

(3) (a) Jambor, R.; Dostál, L.; Růžička, A.; Císařová, I.; Brus, J.; Holčapek, M.; Holeček, J. *Organometallics* **2002**, *19*, 3996. (b) Kašná, B.; Jambor, R.; Dostál, L.; Růžička, A.; Císařová, I.; Holeček, J. *Organometallics* **2004**, *23*, 5300. (c) Kašná, B.; Jambor, R.; Dostál, L.; Kolářová, L.; Císařová, I.; Holeček, J. *Organometallics* **2006**, *25*, 148. (d) Mehring, M.; Schürmann, M.; Jurkschat, K. *Organometallics* **1998**, *17*, 1227. (e) Mehring, M.; Loew, C.; Schürmann, M.; Jurkschat, K. *Eur. J. Inorg. Chem.* **1999**, 887. (f) Mehring, M.; Loew, C.; Uhlig, F.; Schürmann, M.; Jurkschat, K.; Mahieu, B. *Organometallics* **2000**, *19*, 4613. (g) Mehring, M.; Vrasidas, I.; Horn, D.; Schürmann, M.; Jurkschat, K. *Organometallics* **2001**, *20*, 4647. (h) Peveling, K.; Henn, M.; Loew, C.; Mehring, M.; Schürmann, M.; Jurkschat, K. *Organometallics* **2004**, *23*, 1501. (i) Dostál, L.; Jambor, R.; Růžička, A.; Lyčka, A.; Holeček, J. *Magn. Reson. Chem.* **2006**, *44*, 171.

(4) Bondi, A. *J. Phys. Chem.* **1964**, *68*, 441.

10.1021/om700576n CCC: $37.00
Publication on Web 11/06/2007

Scheme 1

1, R = Me, M = $SnPh_3$
2, R = Me, M = $SnPh_2Cl$
3, R = Me, M = $SnPhCl_2$
4, R = Et, M = $SnPh_3$
5, R = Et, M = $SnPh_2Cl$
6, R = Et, M = $SnPhCl_2$

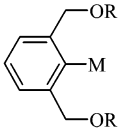

7, R = *i*-Pr, M = $SnPh_3$
8, R = *i*-Pr, M = $SnPh_2Cl$
9, R = *i*-Pr, M = $SnPhCl_2$
10, R = t-Bu, M = $SnPh_3$
11, R = *t*-Bu, M = $SnPh_2Cl$
12, R = *t*-Bu, M = $SnPhCl_2$

(Scheme 1) and attempts to bring them in relationship to Sn−O bond lengths, as determined by XRD techniques and obtained from DFT calculation. The synthesis and X-ray structure of organotin(IV) derivatives (**4**−**6**) (Scheme 1) based on the new O,C,O-chelating ligand $[2,6\text{-}C_6H_3(CH_2OEt)_2]^-$ are presented as well.

Results and Discussion

Solution Study. In the previous study,[3] the solution ^{119}Sn chemical shifts and $^1J(^{13}C-^{119}Sn)$ coupling constants of 9 of the 12 compounds (**1**−**3**, **7**−**12**) indicated similar structural arrangements in solution and in the solid state, but no estimation of the strength of their Sn−O interaction in solution was available. It was believed that measuring long-range $^nJ(^1H-^{119}Sn)$ coupling constants, from 1D[6] and/or 2D[7] ge-^{1}H−^{119}Sn *J*-HMQC spectra, could offer the possibility to obtain this information. The nominal $^4J(^1H-^{119}Sn)$ coupling constants for the benzylic CH_2 protons are reported in Table 1, together with some relevant ^{119}Sn chemical shifts and $^1J(^{13}C-^{119/117}Sn)$ coupling constants of the new compounds, other previously studied ones,[3] and a reference compound without pincer ligand,[8] reported for comparison. The triphenyltin derivatives, when compared to the reference compound, display a chemical shift to lower frequency by some 25−35 ppm, due to shielding from neighboring substituents and/or a weak interaction between the tin atom and the oxygen atoms.[8,9] The smallest upfield shift in ^{119}Sn chemical shift and smallest increase in $^1J(^{13}C-^{119/117}Sn)$ coupling constant with respect to tetraphenyltin are observed for compound **10**, with the bulky *t*-butyl-group on the oxygen atom. Because solid-state data of **10** (see below) show the absence of interaction between the tin atom and the oxygen atoms, the increased shielding in chemical shift of **10** with respect to the reference can be ascribed solely to the steric bulk of the *t*-butyl groups on the oxygen atoms of the pincer. The ^{119}Sn NMR spectra of the other triphenyltin derivatives **1**, **4**, and **7** show slightly increasing negative chemical shifts and increasing couplings upon decreasing bulkiness of the substituent on oxygen, indicating an increasing (but weak) interaction between tin and oxygen, confirmed by the Sn−O distances decreasing concertedly in the solid state (Table S11). The $^4J(^1H-^{119}Sn)$ coupling constants of the benzylic protons increase in the triphenyltin series with increasing size of the substituent on oxygen. This can be ascribed either to the increasing electronegativity of the oxygen atom bound to these benzylic protons (see Table S7, Supporting Information, where the O atomic charge appears highest for R = *t*-Bu) or to the contribution of an increasing interaction with tin, resulting in a second coupling pathway over three bonds with $^3J(^1H-^{119}Sn)$ coupling constant of opposite sign.

The low- and room-temperature spectra of these compounds are very similar. However, compound **1** has a slightly smaller benzylic $^4J(^1H-^{119}Sn)$ coupling constant (4.7 as compared to 5.6 Hz), in line with the proposal of the contribution of a second pathway with coupling constant of opposite sign logically increasing at lower temperature as the O→Sn interaction becomes stronger.

The ^{119}Sn NMR spectra of the chlorodiphenyltin compounds **2**, **5**, **8**, and **11** show a more pronounced shift to higher field of 80−100 ppm, when compared to triphenyltin chloride, characteristic for coordination expansion by one ligand, as confirmed by a $^1J(^{13}C-^{119}Sn)$ coupling increase of about 100 Hz. This coordination expansion, by interaction of the tin atom with alternatively one of the ligand oxygen atoms, is due to the increased Lewis acidity of the tin atom upon substitution of one phenyl substituent by a chlorine atom. The *t*-Bu group in **11** does not prevent this interaction, confirming the higher Lewis acidity of tin in the triaryltin chlorides than in the tetraaryl compounds. At room temperature, the same relative trend in chemical shift as in the previous series **1**, **4**, **7**, and **10** reveals again an increasing interaction with decreasing size of the oxygen substituent. The benzylic $^4J(^1H-^{119}Sn)$ couplings all have about the same value, to be interpreted as the result of several changing parameters with opposing but mutually balancing effects. First, a coupling increase is expected as a consequence of the presence of the electronegative chlorine atom on the tin atom. Second, the additional coordination between tin and oxygen creates a second scalar ^3J coupling pathway of opposite sign to the ^4J through the benzene ring. Third, the additional coordination can generate a stronger steric repulsion with bulky groups. At low temperature, the ^{119}Sn nuclei are more shielded (Table 2), and the benzylic protons resonances decoalesce into two singlets for compounds **2** and **5**, as the result of the equilibrium in which either of the oxygen atom coordinates the tin atom, slowing down. For the *t*-butyl derivative, **11**, and the *i*-propyl one, **8**, decoalescence is not yet complete at −80 °C.[3] At this temperature, the $^nJ(^1H-^{119}Sn)$ coupling constants for the two benzylic protons of **2** (9.8 and 10.5 Hz) and **5** (12.6 and 13.1 Hz) are both higher than at room temperature, being higher for the latter ethyl than the former methyl derivative, in contrast to room temperature. These data match the expected strengthened coordination at lower temperature, the slightly higher value of the ethoxy group being compatible with its higher inductive electron-releasing effect than the methoxy group, as supported by the more negative charge of oxygen in the ethoxy versus the methoxy compound (see Table S7, Supporting Information). Thus, the coordination being stronger but the interaction ring configuration being also likely more rigid at lower temperature, the relative weight of both possibly antagonistic effects is difficult to assess.

(5) (a) Jurkschat, K.; Pieper, N.; Seemeyer, S.; Schürmann, M.; Biesemans, M.; Verbruggen, I.; Willem, R. *Organometallics* **2001**, *20*, 868. (b) van Koten, G.; Noltes, J. G. *J. Am. Chem. Soc.* **1976**, *98*, 5393. (c) Jambor, R.; Císařová, I.; Růžička, A.; Holeček, J. *Acta Crystallogr.* **2001**, *C57*, 373. (d) Nath, M.; Yadav, R.; Eng, G.; Musingarimi, P. *Appl. Organomet. Chem.* **1999**, *13*, 29 and references therein. (e) Crowe, A. J. In *Metal Complexes in Cancer Chemotherapy*; Keppler, B. K., Ed.; VCH: Weinheim, Germany, 1993; pp 369−379. (f) Gielen, M.; Lelieveld, P.; de Vos, D.; Willem, R. In *Metal-Based Antitumor Drugs*; Gielen, M., Ed.; Freund Publishing House: Tel Aviv, Israel, 1992; Vol. 2, pp 29−54.

(6) (a) Willem, R.; Bouhdid, A.; Meddour, A.; Camacho-Camacho, C.; Mercier, F.; Biesemans, M.; Ribot, F.; Sanchez, C.; Tiekink, E. R. T. *Organometallics* **1997**, *16*, 4377. (b) Willem, R.; Biesemans, M.; Jaumier, P.; Jousseaume, B. *J. Organomet. Chem.* **1999**, *572*, 233. (c) Martins, J. C.; Biesemans, M.; Willem, R. *Prog. Nucl. Magn. Reson. Spectrosc.* **2000**, *36*, 271.

(7) (a) Biesemans, M.; Martins, J. C.; Willem, R.; Lyčka, A.; Růžička, A.; Holeček, J. *Magn. Reson. Chem.* **2002**, *40*, 65. (b) Biesemans, M.; Martins, J. C.; Jurkschat, K.; Pieper, N.; Seemeyer, S.; Willem, R. *Magn. Reson. Chem.* **2004**, *42*, 776.

(8) (a) Holeček, J.; Nádvorník, M.; Handlíř, K.; Lyčka, A. *J. Organomet. Chem.* **1983**, *241*, 177. (b) Holeček, J.; Nádvorník, M.; Handlíř, K.; Lyčka, A. *Collect. Czech. Chem. Commun.* **1990**, *55*, 1193.

(9) (a) Holeček, J.; Nádvorník, M.; Handlíř, K.; Lyčka, A. *Z. Chem.* **1990**, *30*, 265. (b) Lyčka, A.; Holeček, J.; Schneider, B.; Straka, J. *J. Organomet. Chem.* **1990**, *389*, 29. (c) Pejchal, V.; Holeček, J.; Lyčka, A. *Sci. Univ. Pap. Pardubice* **1996**, *A2*, 35; *Chem. Abstr.* **1997**, *126*, 317445.

Table 1. Selected ^{119}Sn and ^{1}H NMR Data for Compounds 1−12 in $CDCl_3$ Solution at Room Temperature (Chemical Shift in ppm, Coupling Constants in Hz)[a]

	$SnPh_3$		$SnPh_2Cl$		$SnPhCl_2$	
2,6 substituent	δ^{119}Sn [$^1J(^{13}C-^{119}Sn)$]	δ^1H [$^4J(^1H-^{119}Sn)$]	δ^{119}Sn [$^1J(^{13}C-^{119}Sn)$]	δ^1H [$^4J(^1H-^{119}Sn)$]	δ^{119}Sn [$^1J(^{13}C-^{119}Sn)$]	δ^1H [$^4J(^1H-^{119}Sn)$]
CH_2OMe (**1**−**3**)	−164 [571/543]	4.18 [5.6]	−145 [730/734]	4.51 [7.6]	−210 [997/1027]	4.68 [10.9]
CH_2OEt (**4**−**6**)	−160 [560/540]	4.22 [5.9]	−141 [712/737]	4.57 [7.1]	−198 [975/1010]	4.71 [10.5]
CH_2O^iPr (**7**−**9**)	−155 [542/527]	4.30 [7.1]	−136 [684/738]	4.67 [7.2]	−178 [931/996]	4.73 [9.9]
CH_2O^tBu (**10**−**12**)	−156 [536/521]	4.24 [8.0]	−122 [714/721]	4.60 [7.2]	−149 [872/946]	4.71 [9.1]
no subst.	−128 [531]		−45 [614]		−32 [786]	

[a] The first $^1J(^{13}C-^{119}Sn)$ coupling constant refers to the tin-bound ipso carbon atom of the O,C,O-pincer ligand, while the second refers to the tin-bound carbon of the phenyl groups.

Table 2. Selected ^{119}Sn and ^{1}H NMR Data for the Chlorodiphenyltin and Dichlorophenyltin Compounds in CD_2Cl_2 Solution at 193 K (Chemical Shift in ppm, Coupling Constants in Hz)

	$SnPh_2Cl$		$SnPhCl_2$	
2,6 substituent	δ^{119}Sn	δ^1H[a] [$^nJ(^1H-^{119}Sn)$]	δ^{119}Sn	δ^1H[b] [$^nJ(^1H-^{119}Sn)$]
CH_2OMe (**2**,**3**)	−155	4.57 [9.8], 4.23 [10.5]	−228	4.86 [12.4], 4.30 [8.7]
CH_2OEt (**5**,**6**)	−154	4.60 [12.6], 4.27 [13.1]	−213	4.85 [10.7], 4.48 [6.0]
CH_2O^iPr (**8**,**9**)	−163	4.72, 4.41 (broadened)	−198	4.85, 4.44 (broadened)
CH_2O^tBu (**11**,**12**)	−144	4.55 (broadened)	−168	4.89, 4.34 (broad)

[a] Singlet. [b] AX pattern: $^2J(H-H) = 11-12$ Hz.

The ^{119}Sn NMR chemical shifts of the dichlorophenyltin compounds **3**, **6**, **9**, and **12** shift to lower frequencies over 120−180 ppm, when compared to the reference Ph_2SnCl_2 compound, being intermediate shifts for expansion by one and two coordination numbers. The $^1J(^{13}C-^{119/117}Sn)$ couplings increase by 100−220 Hz relative to the reference that confirms this. The difference between the $^1J(^{13}C-^{119/117}Sn)$ couplings of the ipso carbon atom of the O,C,O-pincer ligand and the unsubstituted phenyl group on the tin atom is highest in this series, the strongest s character being concentrated in the tin hybrid atomic orbitals involving tin−carbon bonds. The low-temperature spectra of **3**, **6**, **9**, and **12** display a decoalescence of the benzylic proton singlet into two doublets of an AX pattern, only compatible with a C_2 structure in which both oxygen atoms are coordinated to the tin atom, the two benzylic protons of each of the two homotopic alkoxy substituents being mutually diastereotopic. With this C_2 6-coordinate complex in equilibrium with the open 5-coordinate structure, internal rotation about the C−C bond and the association−dissociation exchange of the two Sn−O bonds become fast on the NMR time scale at room temperature and the chirality of the molecule expressed at low temperature averages out and results in symmetry equivalent protons. This structure is confirmed by X-ray diffraction data and theoretical calculations (see below). The relative differences in chemical shift and coupling constants reflect the mean Sn−O distance, increasing from compound **3** to **12**. The $^nJ(^1H-^{119}Sn)$ coupling constants follow perfectly the $^1J(^{13}C-^{119/117}Sn)$ coupling sequence. At low temperature, the cyclic structure causes the diastereotopic benzylic protons to have different ^3J couplings because they have different dihedral angles, which makes irrelevant comparison with room-temperature values.

Solid-State Structures. The X-ray structures of compounds **5** and **6** were determined. Their crystallographic data are summarized in Table S10 and selected bond distances and angles in Table S11, where these parameters are gathered with computed values (see below) and experimental data published earlier, for the sake of comparison.[3] The geometry of the tetraorganotin compound **10** (Scheme 1)[10] is nearly perfectly tetrahedral, with an average C−Sn−C angle of 109.42° (to be compared with 109.22° for **1**) and 109.46° for the unsubstituted Ph_4Sn[11] analogue, the largest deviation from ideal tetrahedral shape being found for C(11)−Sn−C(41) 118.63° (116.98° for **1** and 111.2° in Ph_4Sn).[10] The Sn−C bond distances are almost identical to the corresponding bond distances in **1**. The strength of the Sn−O interaction is most dramatically different between **1** and **10**. The values of both Sn−O distances (4.538 and 4.799 Å, respectively) indicate a total absence of interaction for **10** (the sum of the van der Waals radii of oxygen and tin is 3.70 Å), which is in striking contrast with **1** where the Sn−O distances (2.908 and 2.966 Å, respectively)[3] do suggest a weak but effective interaction. This result shows again that the strength of the Sn−O bond is strongly influenced by the steric hindrance developed by the substituents on the oxygen atoms of the O,C,O-chelating ligand.[3a−c,h]

The triorganotin compound **5** is a good example of a [3+2]-coordination with a C_3ClOSn-distorted trigonal bipyramid (Figure 1). The central tin atom together with the carbon atoms form an equatorial plane (the sum of the angles for the C−Sn−C girdle is 351.86°), while the chlorine and oxygen atoms are in axial positions (the value of the bonding angle O(1)−Sn−Cl(1) is 179.03(3)°). The value of the Sn−O(1) bond length (2.454(1) Å) is smaller than the sum of the van der Waals radii of oxygen and tin (3.70 Å), but larger than the sum of the covalent radii (2.066 Å), thus indicating the presence of a medium-strong Sn−O interaction in this compound. The second oxygen atom is out of the tin coordination sphere or nearly so (the value of Sn−O(2) bond length is 3.473(1) Å). The mentioned parameters together with the O(1)−Sn−O(2) angle of 113.63(4)° demonstrate a different shape of the tin coordination polyhedron in **5** as compared to **2**.

The diorganotin compound **6** is a characteristic example of a [5+1]-coordination where the distorted C_2Cl_2OSn-trigonal bipyramid is attacked by an oxygen donor atom (Figure 2). The equatorial plane is formed by one chlorine (Cl(2)) and two carbon atoms (the sum of bonding angles for the C_2ClSn girdle is 348.1). The second chlorine atom and the oxygen atom occupy the axial positions, in agreement with the value of the bonding angle O(1)−Sn−Cl(1) of 167.65(3)°. The values of both Sn−O bond lengths (Sn−O(1) 2.447(1) Å and Sn−O(2) 2.864(1) Å) indicate the presence of both medium-strong (Sn−O(1)) and weak interactions (Sn−O(2)) in **6**. However, this weak Sn−O

(10) Dostál, L.; Jambor, R.; Růžička, A.; Jirásko, R.; Císařová, I.; Holeček, J. *J. Organomet. Chem.* **2006**, *691*, 35.

(11) Belsky, V. K.; Simonenko, A. A.; Reikhsfeld, V. O.; Saratov, I. E. *J. Organomet. Chem.* **1983**, *244*, 125.

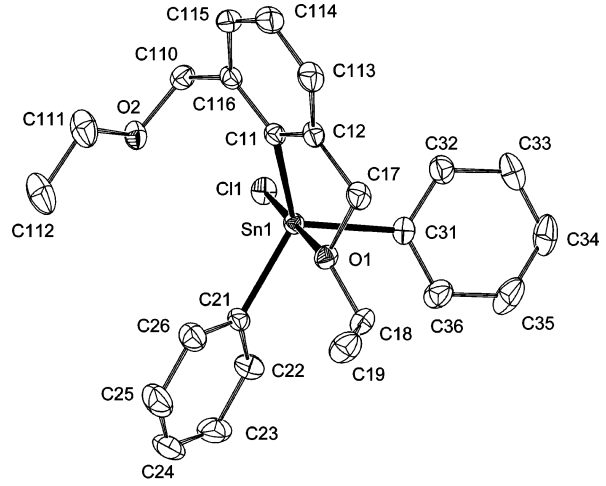

5

Figure 1. General view (ORTEP) of a molecule showing 50% probability displacement ellipsoids and the atom numbering scheme for **5**. The hydrogen atoms are omitted for clarity.

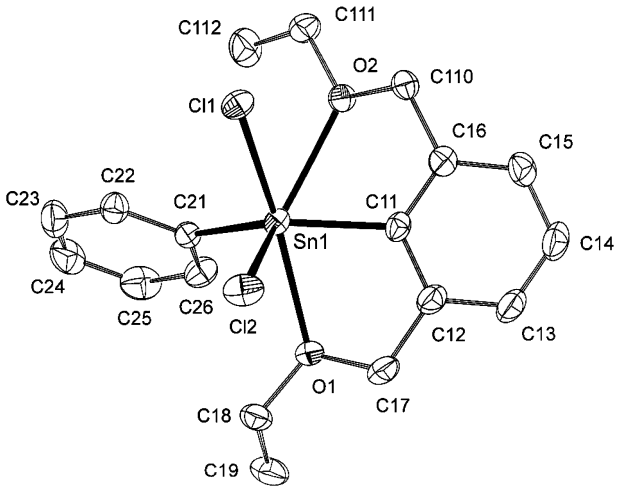

6

Figure 2. General view (ORTEP) of a molecule showing 50% probability displacement ellipsoids and the atom numbering scheme for **6**. Only one molecule from the crystal lattice of **2** without hydrogen atoms has been chosen for clarity.

interaction causes the deformation of the equatorial plane, where the bonding angles (107.6°, 108.9°, and 131.6°) are significantly different from those in an ideal trigonal bipyramid (120°). The value of the bonding angle of O(1)−Sn−O(2) = 118.51(4)° shows that both donor oxygen atoms are mutually in cis position, this value being comparable to those found in the other diorganotin compounds **3**, **9**, and **12**.

Theoretical Calculations. All geometries were optimized at the B3LYP[12]/LANL2DZ[13] level starting from the experimental crystal structural parameters of the compounds. In those cases where no crystal structures were available, starting structures were generated in silico. These structures are given in the Supporting Information (S1). It has been shown that this level of theory is capable of qualitatively describing intramolecular interactions in organotin compounds, including compounds containing pincer ligands.[14]

Table S11 lists geometrical parameters for all of the compounds considered in this work. For the L−$SnPh_3$ compounds **1** (Figure 3), **4**, **7**, and **10**, it can be deduced from the different C−Sn−C bond angles that the geometry of these compounds can be described as a distorted tetrahedron, the average of these angles amounting to 113.1° (R = Me), 113.0° (R = Et), 113.0° (R = *i*-Pr), and 113.4° (R = *t*-Bu). The difference between the two Sn−O bond distances largely increases when going from R = Me to R = *i*-Pr, but decreases again for *t*-Bu, the shortest Sn−O distance decreasing from 2.911 Å for R = Me to 2.664 Å for R = *i*-Pr, indicating an apparent increase of the Lewis acidity of the Sn atom throughout this series. However, while the two Sn−O distances are very different for **4** (R = Et) and **7** (R = *i*-Pr), they are rather similar for **1** (R = Me), in good agreement with experimental X-ray diffraction data for **1** and **10**, not available for **4** and **7**. In all three cases, the local geometry around the Sn atom could also be described as a distorted trigonal bipyramid, even though the different relevant angles deviate substantially from the ideal trigonal bipyramid angles. For the *t*-Bu compound **10**, however, the two Sn−O bond distances are substantially longer than 3 Å, but shorter than the sum of the van der Waals radii, 3.70 Å, indicating a weak contact in strong contrast with the experimental values. The excellent agreement between the experimental and calculated values is especially noticeable for **1**, while discrepancies observed for **10** appear mostly in all distances and bond angles involving either oxygen atom O(1) or O(2). While this is most likely related, at least in part, to specific packing effects and geometry distortions arising from the bulky *t*-Bu group in the crystalline state, it can likewise be suggested that in silico, where in principle gas-phase structures are reflected and crystal packing effects should be absent, very weak potential wells related to attractive O→Sn interactions still can exist and contribute to the overall stability of compound **10**. It thus appears that these kinds of calculations have a good predictive value for the geometrical parameters in the crystalline state in structural situations where the substituents on the coordinating oxygen atoms of the pincer ligand are not too sterically demanding. It should be stated that the absence of any supramolecular structure resulting from intermolecular aggregation largely contributes to this conclusion. Globally, among the four tetraaryl compounds **1**, **4**, **7**, and **10**, the one with R = Me, **1**, can be considered as having a 4-coordinate tin atom, with a weak symmetrical extension to 6-coordination, so that **1** can be considered as a compound with symmetrical "4 + 2"-coordination. The ones with R = Et and *i*-Pr, **4** and **7**, respectively, have one stronger and one weaker coordination expansion, when compared to **1**, which make them to be considered as compounds with nonsymmetrical "4 + 2"-coordination, or alternatively "4 + 1"-coordination if the weaker interaction corresponding to a contact distance between Sn and O of 3.3 Å or even more is neglected. Compound **10** would then have, in these pictures, either a weak symmetric "4 + 2"-coordination, both Sn−O contacts around 3.3 Å being in silico of the same order in **10** as in **4** and **7**, or basically a standard 4-coordination.

Also, in the case of the L-$SnPh_2Cl$ compounds **2**, **5**, **8**, and **11**, there is a considerable difference between the two Sn−O bond distances. From the data, it can be seen that these structures

(12) (a) Becke, A. D. *J. Chem. Phys*. **1993**, *98*, 5648. (b) Lee, C.; Yang, W.; Parr, R. G. *Phys. Rev. B* **1988**, *37*, 785. (c) Stevens, P. J.; Delvin, F. J.; Chablaoski, C. F.; Frisch, M. J. *J. Phys. Chem.* **1994**, *98*, 11623.

(13) Wadt, W. R.; Hay, P. J. *J. Chem. Phys*. **1985**, *82*, 270.

(14) (a) Buntine, M. A.; Hall, V. J.; Kosovel, F. J.; Tiekink, E. R. T. *J. Phys. Chem. A* **1998**, *102*, 2472. (b) Ryner, M.; Finne, A.; Albertsson, A.-C.; Kricheldorf, H. R. *Macromolecules* **2001**, *34*, 7281. (c) Obora, Y.; Nakanishi, M.; Tokunaga, M.; Tsuji, Y. *J. Org. Chem.* **2002**, *67*, 5835. (d) Hu, Y.-H.; Su, M.-D. *J. Phys. Chem. A* **2003**, *107*, 4130. (e) Peveling, K.; Henn, M.; Löw, C.; Mehring, M.; Schürmann, M.; Costisella, B.; Jurkschat, K. *Organometallics* **2004**, *23*, 1501. (f) Fischer, J.; Schürmann, M.; Mehring, M.; Zachwieja, U.; Jurkschat, K. *Organometallics* **2006**, *25*, 2886.

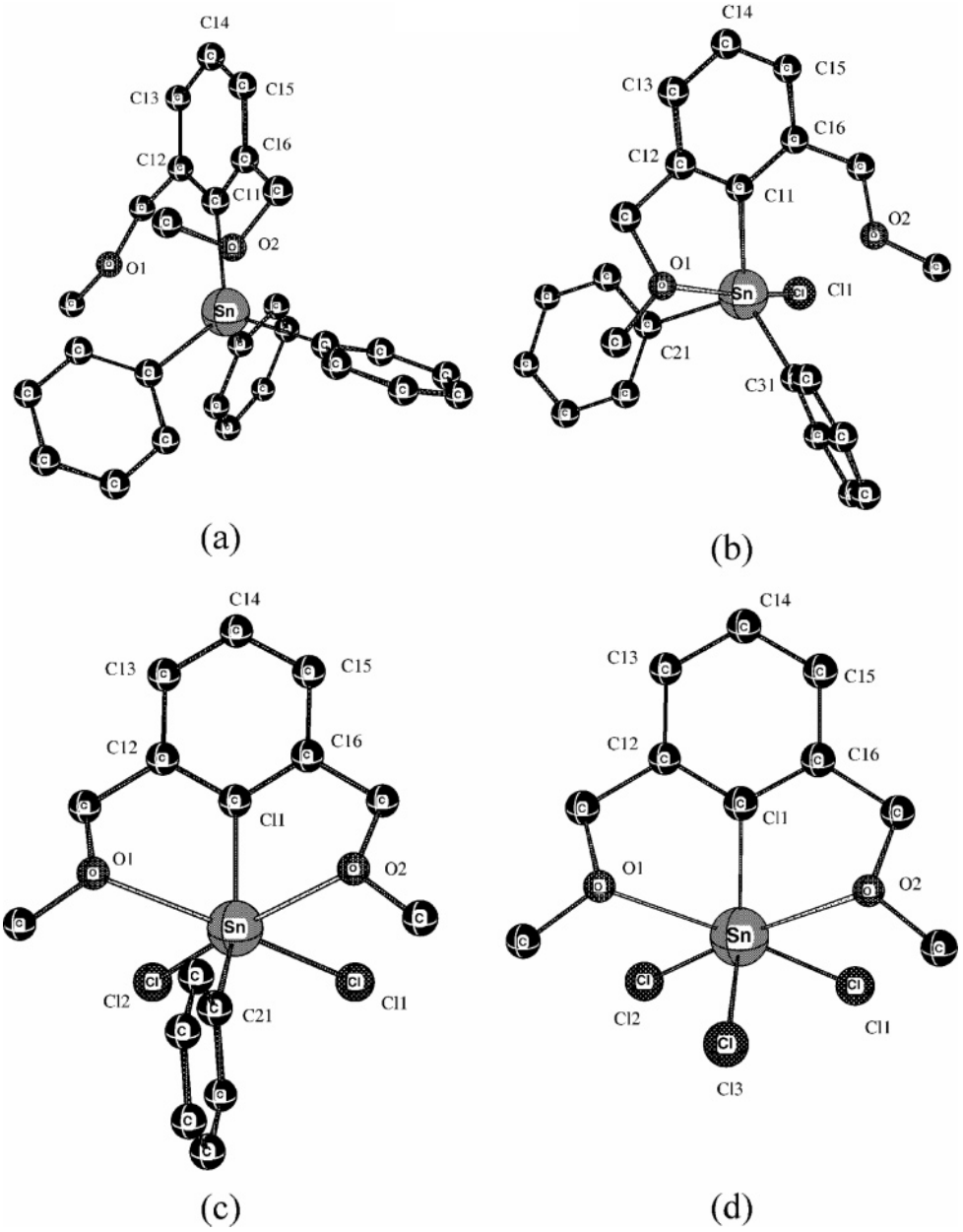

Figure 3. Computed molecular models of the methyl derivative of the L−$SnPh_3$ (**1**), L−$SnPh_2Cl$ (**2**), L−$SnPhCl_2$ (**3**), and L−$SnCl_3$ compounds studied in this work.

can generally be described as a distorted trigonal bipyramid, the chlorine and the alkoxy substituents taking the axial positions. The ipso-carbon−Sn−Cl angle averages to about 106° (103.1° in the case of the *t*-Bu compounds), thus showing a deviation of around 16° from the angle in a perfect trigonal bipyramid toward the tetrahedral geometry. The angles between the axial compounds range from 160.4° (for R = *i*-Pr) to 172.1° (for R = Et). Finally, the interaction of the second alkoxy group with the Sn atom is generally smaller but not negligible in the case of R = Me, which is in line with the considerable deviations of the bond angles around the tin atom with respect to the ideal trigonal bipyramid. Again, the agreement between experimental and calculated data is excellent for **2**, with R = Me, but less for **5**. Table S11 shows globally that the calculated bond lengths and angles for **8** and **11** have a satisfactory predictive value, because they are in global good agreement with the corresponding geometrical parameters of compounds **2** and **5** for which the agreement between experimental X-ray diffraction data and computed values is likewise satisfactory. While the non-symmetry in the Sn−O contacts is of variable degree, with a distance difference of at least ca. 0.35 Å (R = Me, **2** and R = *i*-Pr, **8**), and even greater for R = Et, **5** (ca. 0.6−0.7 Å), or dramatically more for R = *t*-Bu, **11**, this non-symmetry reflects the higher degree of stability of the "3 + 2"-coordination characteristic for triorganotin monohalides undergoing a rather strong coordination expansion by any oxophilic ligand, where the three organic groups occupy the equatorial and the nucleophilic or electronegative substituents occupy the axial, mutually trans positions of the usual distorted trigonal bipyramidal configuration of the metal atom. This explains why the symmetrical "4 + 2"-coordination is not favored, despite the second intramolecular oxygen containing ligand. Note nevertheless that the contact between the second oxygen containing ligand and the tin, of the order of 2.9−3.1 Å, remains by far lower than the sum of the van der Waals radii of tin and oxygen, so that a weaker, non-symmetrical "4 + 2"-coordination can also be considered for **2**, **5**, and **8**.

Next, for the geometrical parameters of the L−$SnPhCl_2$ compounds **3**, **6**, **9**, and **12**, in the case of R = Et, **6**, and R = *i*-Pr, **9**, the asymmetry in the Sn−O bond distances is large, whereas for the Me and *t*-Bu compounds, these are equal. This duality is remarkably self-consistent in the X-ray data and the theoretical calculations, confirming the high predictive value of the latter in this series of compounds. This can be ascribed to the Lewis acidity factor being so dominant that computational deviations related to steric hindrance are faded away. All of the structures can be considered as heavily distorted octahedra. In all four compounds **3**, **6**, **9**, and **12** of Table S11, the two ipso-carbon−Sn−Cl angles deviate from 90° toward the tetrahedral angle. Because, however, in all cases the Sn−O contacts appear shorter than 3 Å, compounds **3**, **6**, **9**, and even **12**, with R = *t*-Bu, can be considered to be of a stable and strong "4 + 2" type.

Finally, for the L−$SnCl_3$ compounds, for which, apart from R = Me, no X-ray diffraction data are available, the two Sn−O distances are virtually equal for R = Me, whereas the asymmetry in these distances increases upon increasing alkyl group size. These compounds can again be considered to be heavily distorted octahedra with a typical distorted "3 + 3" 6-coordination of the type R_3SnCl_3 with a *fac* configuration for the three chlorine atoms, as evidenced by the fact that none of the Cl−Sn−Cl bonds deviates by more than 15° from the ideal 90° one, one of the Cl−Sn−Cl angles for a *mer* configuration being 180°. Again, the comparison between the calculated and the experimental X-ray data for R = Me shows the good predictive value of the calculations. Because globally the corresponding values for R = Et and R = *i*-Pr are rather similar, it can be concluded that the corresponding in silico structures should properly predict the actual structure of these compounds. For R = *t*-Bu, no optimum could be found in the calculation, a dissociation being obtained during the optimization, explaining why no computational data are provided for this case.

For the various compounds considered in this work, it can be assumed that the strength of the oxygen−tin interactions observed can be inversely correlated to the observed bond lengths between these atom pairs. As can be seen from the data in Table S11, the majority of Sn−O distances are substantially shorter than the sum of the van der Waals radii of the Sn and O atoms, but also significantly longer than the sum of their covalent radii. These interactions between the nucleophilic oxygen atom and the electrophilic tin atom thus vary from weak to moderately strong. The O−Sn bond distances decrease upon increasing number of chlorine atoms on the central tin atom. Moreover, the two oxygen−tin bond distances tend to equalize upon increasing the number of chlorine atoms, in agreement with the experimentally measured distances, meaning that the degree of 6-coordination increases upon increasing the number of chlorine atoms. For the $SnPhCl_2$ and the $SnCl_3$ compounds, 6-coordination is clear-cut. In general, when going from the methyl to the *t*-butyl-substituted compounds, the difference between the oxygen−tin bond distances increases. When focusing on the smaller of these two distances, the lower values are observed systematically for the *i*-propyl compounds, the only exception being the triorganotin chloride series. These general trends match also pretty well the NMR data in solution, even though it appears difficult to give an accurate interpretation of the nominal $^4J(^{119}Sn-^1H)$ long-range couplings, because the scalar coupling values observed reflect necessarily the average of the differences in Sn−O interactions observed in the crystalline state and in silico, and, more importantly, because these long-range coupling constants raise from two different coupling pathways displaying opposite signs, and involving an actual ^4J "organic" H−C−C−C−Sn coupling pathway through only C−Sn and C−C bonds, and another ^3J "coordinative" H−C−O−Sn pathway, the latter being itself the average of two mostly non-symmetry equivalent ones and involving coordinative Sn−O bonds of increasing averaged strength as the number of chlorine atoms increases.

Details of an investigation using density functional theory based descriptors,[15] aiming at gaining further insight into such trends in the oxygen−tin bond distances, are presented in the Supporting Information (S2), together with tin atomic charges in the various compounds.

From this analysis, it could be concluded that the combination of moieties with the highest Lewis acidity for the tin atom and basicity for the oxygen atom yields the compound with the shortest O−Sn distance (Table S11), that is, the trichlorotin compound with R = *i*-Pr.

Conclusion

This work proposes an integrated approach for structural investigations of organotin molecules of the type $LSnPh_{(3-n)}Cl_n$, where L represents an aromatic O,C,O-pincer ligand with two oxygen donors potentially able to interact with the tin atom toward coordination expansion of the tin atom. The combined use of X-ray diffraction in the crystalline state, NMR measurements of heteronuclear long-range $^1H-^{119}Sn$ coupling constants involving dual coupling pathways in solution, and structural parameter determinations of isolated molecules in silico provides complementary information on these compounds in three aggregation states. For a constant number of chlorine atoms on the tin atom, the strength of the interaction of the Sn−O contacts appears to be extremely sensitive to the substituent on the oxygen atoms, which influences in particular the symmetry equivalence or not of these two Sn−O contacts. For the tetraaryltin compounds, the coordination at tin turns out to vary mainly from the weak "4 + 2"- to pure 4-coordination state when going from Me to *t*-Bu substitution on the potentially coordination oxygen atoms. For the monochlorotriorganotins, the general trend is mainly to a "3 + 2"-coordination of a distorted trigonal bipyramid with triequatorial arrangement of the organic ligands, with, however, strong differences between the two O−Sn coordinative interactions, allowing an alternative weak "4 + 2"-coordination for some of the compounds. The dichlorodiorganotins have clear-cut, strong 6-coordination in which the two organic aryl ligands have a configuration lying slightly closer to the cis than the theoretically ideal trans one, confirming the major coordination distortion induced by the O,C,O-pincer ligand. The trichloromonoorganotins have likewise clear-cut, strong 6-coordination with the three chlorine atoms displaying the most pincer ligand strain releasing *fac* configuration.

For the assessment of the increasing strength of the donor−acceptor O−Sn interactions, the combined use of X-ray diffraction for the crystalline state, NMR long-range coupling constants in solution, and ab initio calculations for simulating the gas phase turned out to be powerful in providing concurrent data evidencing that these interactions do not significantly depend on the aggregation state, but, rather, are highly sensitive to both the substitution pattern on tin and even more, in part unexpectedly, to the substitution pattern of the coordinating oxygen atoms.

(15) Geerlings, P.; De Proft, F.; Langenaeker, W. *Chem. Rev.* **2003**, *103*, 1793.

Experimental Section

General Methods. All solvents were dried by standard procedures and distilled prior to use. All reactions were carried out under purified argon atmosphere using standard Schlenk techniques.

^{1}H and ^{119}Sn NMR spectra were recorded for long-range coupling constant measurements in $CDCl_3$ and CD_2Cl_2 at 303 and 193 K on a Bruker AMX500 instrument, operating at frequencies of 500.13 and 186.47 MHz for ^{1}H and ^{119}Sn nuclei, respectively. Routine characterizations were performed on a Bruker AMX 360 instrument, operating at frequencies of 360.13, 90.14, and 134.27 MHz for ^{1}H, ^{13}C, and ^{119}Sn nuclei, respectively. ^{1}H chemical shifts were referenced to the residual solvent peak and converted to the standard TMS scale by adding 5.32 and 7.24 ppm, for CD_2Cl_2 and $CDCl_3$, respectively. For ^{119}Sn nuclei, external referencing was used with $\Xi = 37.290665$ MHz.[16] 1D ge-^{1}H−^{119}Sn HMQC experiments[6] and 2D ge-^{1}H−^{119}Sn *J*-HMQC spectra were recorded as previously described.[7]

In the mass spectrometry, the positive-ion electrospray ionization ESI mass spectra were measured on an Esquire3000 ion trap analyzer (Bruker Daltonics, Bremen, Germany) in the range *m*/*z* 100−1000, and negative-ion ESI mass spectra were measured on the Platform quadrupole analyzer (Micromass, UK) in the range *m*/*z* 15−600. The ion trap was tuned to give an optimum response for *m*/*z* 500. The samples were dissolved in acetonitrile and analyzed by direct infusion at a flow rate of 1−3 μL/min.

Synthetic Procedures. 1,3-Bis(ethoxymethyl)benzenes, **1**−**3**, **7**−**12**, were prepared according to literature procedures.[3a]

[2,6-Bis(ethoxymethyl)phenyl](triphenyl)tin (4). An equimolar amount of 4 mL of *n*-BuLi (1.60 M, 6.4 mmol) was added dropwise at ambient temperature to a solution of 1,3-bis(ethoxymethyl)-benzene (1.23 g, 6.34 mmol) in *n*-hexane (25 mL); the resulting yellow solution was stirred for an additional 2 h. The resulting solution was added dropwise to a suspension of Ph_3SnCl (2.44 g, 6.34 mmol) in 30 mL of *n*-hexane at room temperature, followed by stirring for another 12 h. The resulting solid was filtered and washed with 15 mL of *n*-hexane; the filtrate was concentrated to 15 mL. Crystallization at −10 °C and filtration afforded **4** as a white solid. Yield: 2.4 g (70%), mp 105−108 °C. Anal. Calcd for $C_{30}H_{32}O_2Sn$ (MW 543.28): C, 66.23; H, 5.94. Found: C, 66.52; H, 5.81. MW 544. MS: *m*/*z* 567, 100%, $[M + Na]^+$; 583, 56%, $[M + K]^+$. ^{1}H NMR ($CDCl_3$, 360.13 MHz): δ (ppm) 0.75 (t, 6H, CH_3), 2.87 (q, 4H, OCH_2), 4.23 (s, 4H, CH_2O), 7.31−7.69 (complex pattern, 18H, $SnPh_3$, SnC_6H_3). ^{13}C NMR ($CDCl_3$, 90.14 MHz): δ (ppm) 14.4 (*C*H$_3$), 65.2 (O*C*H$_2$), 74.1 (*C*H$_2$), SnC_6H_3, 136.8 (C(1), $^1J(^{119}Sn,^{13}C = 560.0$ Hz), 128.0, 128.9, 147.1; SnPh, 142.1 (C′(1), $^1J(^{119}Sn,^{13}C = 539.8$ Hz), 128.0, 128.2, 136.8. ^{119}Sn NMR ($CDCl_3$, 134.27 MHz): δ (ppm) −159.

[2,6-Bis(ethoxymethyl)phenyl](chlorodiphenyl)tin (5). Procedure analogous to **4**: 1.15 g, 5.92 mmol of 1,3-bis(ethoxymethyl)-benzene, 3.7 mL, 5.92 mmol of *n*-BuLi 1.60 M, 2.04 g, 5.92 mmol of Ph_2SnCl_2. Yield: 2.0 g (68%), mp 105−107 °C. Anal. Calcd for $C_{24}H_{27}ClO_2Sn$ (MW 501.62): C, 57.47; H, 5.43; Cl, 7.07. Found: C, 57.56; H, 5.92; Cl, 7.25. MW 502. MS: *m*/*z* 467, 100%, $[M - Cl]^+$. ^{1}H NMR ($CDCl_3$, 360.13 MHz): δ (ppm) 0.72 (t, 6H, CH_3), 3.21 (q, 4H, OCH_2), 4.59 (s, 4H, CH_2O), 7.24−7.74 (complex pattern, 13H, $SnPh_2Cl$, SnC_6H_3). ^{13}C NMR ($CDCl_3$, 90.14 MHz): δ (ppm) 13.9 (*C*H$_3$), 66.0 (O*C*H$_2$), 72.3 (*C*H$_2$), SnC_6H_3, 135.5 (C(1), $^1J(^{119}Sn,\ ^{13}C = 712.1$ Hz), 127.1, 129.0, 146.4; SnPh, 142.7 (C′-(1), $^1J(^{119}Sn,\ ^{13}C = 736.8$ Hz), 128.3, 129.0, 135.5. ^{119}Sn NMR ($CDCl_3$, 134.27 MHz): δ (ppm) −140.

[2,6-Bis(ethoxymethyl)phenyl](dichlorophenyl)tin (6). Procedure analogous to **4**: 1.45 g, 7.47 mmol of 1,3-bis(ethoxymethyl)-benzene, 4.7 mL, 7.52 mmol of *n*-BuLi 1.60 M, 2.22 g, 7.47 mmol of $PhSnCl_3$. Yield: 2.7 g (79%), mp 98−100 °C. Anal. Calcd for $C_{18}H_{22}Cl_2O_2Sn$ (MW 459.97): C, 47.00; H, 4.82; Cl, 15.42. Found: C, 46.95; H, 5.21; Cl, 15.63. MW 460. MS: *m*/*z* 483, 3%, $[M + Na]^+$; *m*/*z* 425, 100% $[M - Cl]$. ^{1}H NMR ($CDCl_3$, 360.13 MHz): δ (ppm) 0.79 (t, 6H, CH_3), 3.50 (q, 4H, OCH_2), 4.73 (s, 4H, CH_2O), 7.20−7.85 (complex pattern, 8H, $SnPhCl_2$, SnC_6H_3). ^{13}C NMR ($CDCl_3$, 90.14 MHz): δ (ppm) 13.6 (*C*H$_3$), 66.3 (O*C*H$_2$), 70.4 (*C*H$_2$), SnC_6H_3, 133.4 (C(1), $^1J(^{119}Sn,\ ^{13}C = 975.0$ Hz), 126.2, 130.0, 144.9; SnPh, 142.2 (C′(1), $^1J(^{119}Sn,\ ^{13}C = 1009.9$ Hz), 128.6, 130.4, 134.7. ^{119}Sn NMR ($CDCl_3$, 134.27 MHz): δ (ppm) −197.

Crystallography. Crystals suitable for X-ray structure determination were obtained by vapor diffusion of *n*-hexane into the 5% dichloromethane solutions of compounds **5**, **6**. Data for colorless crystals were collected at 150(2) K on a Nonius KappaCCD diffractometer using Mo Kα radiation ($\lambda = 0.71073$ Å), with a graphite monochromator. The structures were solved by direct methods (SIR92) and refined on F^2 by full-matrix least-squares technique (SHELXL97). Hydrogen atoms were recalculated into idealized positions (riding model) and assigned temperature factors $H_{iso}(H) = 1.2U_{eq}$ (pivot atom) or $1.5U_{eq}$ for the methyl moiety. Absorption corrections were carried out using multiscan procedure (PLATON, SORTAV). From the last cycle of refinement of both structures it follows that $(\Delta/\delta)_{max} < 0.002$. Crystallographic data for individual structures are summarized in Table S10. The experimental standard deviations for all compounds are within intervals: bond type Sn−C ⟨0.0015,0.0030⟩; Sn−Cl ⟨0.0004,0.0009⟩; Sn−O ⟨0.0012,0.0020⟩ Å; bond angle around Sn ⟨0.01,0.11⟩°; torsion angles C−C−C−O ⟨0.1−0.3⟩°.

Crystallographic data for structural analysis have been deposited with the Cambridge Crystallographic Data Centre, CCDC no. 604290 for **5** and 604291 for **6**. Copies of this information may be obtained free of charge from The Director, CCDC, 12 Union Road, Cambridge CB2 1EY, UK (fax, +44-1223-336033; e-mail, deposit@ccdc.cam.ac.uk; or website http://www.ccdc.cam.ac.uk).

Computations. All geometries were optimized at the B3LYP[12]/LANL2DZ[13] level starting from the experimental crystal structures of the compounds using the Gaussian 03 program.[17]

Acknowledgment. The Pardubice group would like to thank the Grant Agency of the Czech Republic (grant no. 203/07/0468) and the Ministry of Education of the Czech Republic (VZ 0021627501) for financial support. The Brussels group wishes to acknowledge the Fund for Scientific Research Flanders (Belgium) (FWO (grants G.0016.02, G.0469.06 (R.W., M.B.)), the Research Council (Onderzoeksraad) of the Vrije Universiteit Brussel (Concerted Research Action, grant GOA31), and the Free University of Brussels (VUB) for continuous support to their research group.

Supporting Information Available: The in silico generated starting geometries for the geometry optimizations, further insights

(16) *Multinuclear NMR*; Mason, J., Ed.; Plenum Press: New York and London, 1987; Appendix p 623.

(17) Frisch, M. J.; Trucks, G. W.; Schlegel, H. B.; Scuseria, G. E.; Robb, M. A.; Cheeseman, J. R.; Montgomery, J. A., Jr.; Vreven, T.; Kudin, K. N.; Burant, J. C.; Millam, J. M.; Iyengar, S. S.; Tomasi, J.; Barone, V.; Mennucci, B.; Cossi, M.; Scalmani, G.; Rega, N.; Petersson, G. A.; Nakatsuji, H.; Hada, M.; Ehara, M.; Toyota, K.; Fukuda, R.; Hasegawa, J.; Ishida, M.; Nakajima, T.; Honda, Y.; Kitao, O.; Nakai, H.; Klene, M.; Li, X.; Knox, J. E.; Hratchian, H. P.; Cross, J. B.; Bakken, V.; Adamo, C.; Jaramillo, J.; Gomperts, R.; Stratmann, R. E.; Yazyev, O.; Austin, A. J.; Cammi, R.; Pomelli, C.; Ochterski, J. W.; Ayala, P. Y.; Morokuma, K.; Voth, G. A.; Salvador, P.; Dannenberg, J. J.; Zakrzewski, V. G.; Dapprich, S.; Daniels, A. D.; Strain, M. C.; Farkas, O.; Malick, D. K.; Rabuck, A. D.; Raghavachari, K.; Foresman, J. B.; Ortiz, J. V.; Cui, Q.; Baboul, A. G.; Clifford, S.; Cioslowski, J.; Stefanov, B. B.; Liu, G.; Liashenko, A.; Piskorz, P.; Komaromi, I.; Martin, R. L.; Fox, D. J.; Keith, T.; Al-Laham, M. A.; Peng, C. Y.; Nanayakkara, A.; Challacombe, M.; Gill, P. M. W.; Johnson, B.; Chen, W.; Wong, M. W.; Gonzalez, C.; Pople, J. A. *Gaussian 03*, revision B.03; Gaussian, Inc.: Wallingford, CT, 2004.

into the observed trends in Sn−O distances, and crystallographic data for **5** and **6** (CIF), as well as the experimental and computed values of selected geometrical parameters of L−$SnPh_3$, L−$SnPh_2$-Cl, L−$SnPhCl_2$, and L−$SnCl_3$. This material is available free of charge via the Internet at http://pubs.acs.org.

OM700576N